

Fractional Precipitation of Rare Earths with Phosphoric Acid

GEOLOGICAL SURVEY BULLETIN 1036-N



Fractional Precipitation of Rare Earths with Phosphoric Acid

By M. K. CARRON, C. R. NAESER, H. J. ROSE, Jr., and F. A. HILDEBRAND

CONTRIBUTIONS TO GEOCHEMISTRY

GEOLOGICAL SURVEY BULLETIN 1036-N

*An application of the study
to the geochemistry
of monazite and xenotime*



UNITED STATES DEPARTMENT OF THE INTERIOR

FRED A. SEATON, *Secretary*

GEOLOGICAL SURVEY

Thomas B. Nolan, *Director*

CONTENTS

	Page
Abstract.....	253
Introduction.....	253
Acknowledgment.....	254
Syntheses of cerium and yttrium phosphates.....	255
Fractional phosphate precipitation of pairs of rare-earth elements.....	256
Methods of preparation.....	256
Separation factors.....	257
Spectrochemical determinations.....	258
Preparation of standards.....	258
Apparatus and operating conditions.....	258
Line pairs.....	259
Precision and accuracy.....	261
X-ray determinations.....	263
Results.....	268
Discussion of results.....	270
Literature cited.....	274

ILLUSTRATIONS

FIGURE 44. A typical working curve of the rare-earth pairs.....	260
45. Variation of separation factors.....	272

TABLES

TABLE 1. Hydrothermal mineral syntheses.....	255
2. Rare-earth line pairs and the intensity ratios of the standards..	261
3. Precision of spectrochemical determinations.....	262
4. Analyses of synthetic unknowns.....	262
5. Spectrochemical analyses and phases produced from fractionally precipitated lanthanide phosphate pairs.....	263
6. X-ray powder diffraction data for synthetic and natural rare-earth phosphates.....	264
7. Hydrothermal syntheses of some single rare-earth phosphates..	269
8. Spectrochemical analyses of fractionally precipitated yttrium and some lanthanide phosphates.....	270

CONTRIBUTIONS TO GEOCHEMISTRY

FRACTIONAL PRECIPITATION OF RARE EARTHS WITH PHOSPHORIC ACID

By M. K. CARRON, C. R. NAESER, H. J. ROSE, JR., and F. A.
HILDEBRAND

ABSTRACT

A study of the fractional precipitation of the phosphates of pairs of adjacent and some nonadjacent rare-earth elements was made by means of wet-chemical, spectrographic, and X-ray powder diffraction techniques. The order of preferential precipitation in adjacent pairs of lanthanide phosphates was found to be La < Ce < Pr < Nd < Sm > Eu > Gd < Tb < Dy < Ho < Er < Tm < Yb > Lu. Samarium was found to precipitate preferentially to all the lanthanides of the cerium subgroup; ytterbium to all the yttrium subgroup; yttrium to Ce, Sm, Eu, and Gd of the cerium subgroup and to dysprosium of the yttrium subgroup, and it may be assumed, therefore, to precipitate preferentially to all the lanthanides of the cerium subgroup. In this study it was found that paired phosphates in the cerium subgroup (lanthanum to gadolinium) had the monazite structure, whereas the paired phosphates in the yttrium subgroup (dysprosium to lutetium) had the xenotime structure. In the interval comprising gadolinium, terbium, and dysprosium (the transition zone), both the monazite and xenotime phases were present in these paired phosphates. The results of this study yield information regarding the paragenesis and composition of the rare-earth phosphate minerals.

INTRODUCTION

Recent chemical and spectrochemical analyses by the United States Geological Survey (Murata and others, 1953, 1957) showed a natural fractionation of the rare-earth elements. Considerable variation in the proportion of the rare earths was found, and it was shown that this could be related to progressive differentiation. This study of fractional precipitation of adjacent pairs of the lanthanides as phosphates was expected to provide information regarding the distribution of individual lanthanides, and also, the possible mode of formation, and order of crystallization and deposition of the phosphate minerals.

Solubility and fractional precipitation studies of the lanthanides in such systems as the oxalate (Weaver, 1954c), bromate, sulfate, and dimethyl phosphate (Yost and others, 1947) are reported in the litera-

ture, indicating different orders of preferential precipitations. These studies were undertaken primarily for their possible application to the development of techniques for separating and purifying some of the lanthanides. The fractional precipitation studies of the lanthanide phosphates presented in this paper were undertaken to obtain fundamental information relating to the geochemistry of rare-earth phosphate minerals, such as monazite and xenotime.

A wet-chemical technique was devised for synthesizing single and paired lanthanide phosphates and yttrium phosphate, which are isostructural with the minerals monazite or xenotime or mixed phases of these. The paired lanthanides form an isomorphous solid-solution series of the type $(A_xB_y)PO_4$, where A and B represent adjacent lanthanides, for example, (La, Ce), (Ce, Pr), (Pr, Nd), and so on; and x and y are values that indicate the degree of preferential precipitation as determined by analyses of the solutions and precipitates. This study is concerned mainly with the ratio $x:y$.

In the present work the term "lanthanide" refers to the elements having atomic numbers 57 to 71, inclusive, whereas the term "rare-earth elements" is used to include yttrium.

In the lanthanide series the paired elements comprising the interval from lanthanum to gadolinium are referred to as the cerium subgroup, whereas those pairs comprising the interval from dysprosium to lutetium are referred to as the yttrium subgroup. The interval comprising the paired lanthanides of gadolinium, terbium, and dysprosium is defined as the transition zone.

Those phases that were found to be isostructural with monazites or xenotimes will be referred to as monazite or xenotime, despite the fact that only one or two lanthanides may be present, in contrast to the natural monazites and xenotimes which may contain a dozen or more lanthanides.

The word "reversal" as used in this paper serves to indicate those points where a salt of a heavier lanthanide shows greater solubility than the similar salt of the adjacent lighter lanthanide and thereby gives a separation factor of a value less than unity.

Weight ratios of the heavier to the lighter rare earths were calculated from their oxides. For example, the weight ratios

$$\frac{\text{weight of Ce}_2\text{O}_3}{\text{weight of La}_2\text{O}_3}, \quad \frac{\text{weight of Sm}_2\text{O}_3}{\text{weight of Y}_2\text{O}_3},$$

and so on, will be referred to below simply as Ce:La, Sm:Y, and so on.

ACKNOWLEDGMENT

We are greatly indebted to our colleague, K. J. Murata, for suggesting the study and for numerous stimulating discussions throughout

the course of this work. With particular reference to the section on "Discussion of results," his interest and close cooperation enabled us to arrive at several geochemical relations.

SYNTHESES OF CERIUM AND YTTRIUM PHOSPHATES

Monazite, essentially monoclinic $(\text{Ce, La}) \text{PO}_4$, and xenotime, tetragonal YPO_4 , have been synthesized by fusion methods (Palache and others, 1951, p. 691, 695). However, to study and evaluate precipitations in the rare-earth phosphate system in relation to natural mineral formation, it seemed more desirable to synthesize these minerals hydrothermally by crystallization from aqueous solution in a closed system. The method used in the syntheses of monazite and xenotime is described under the section on "Fractional phosphate precipitation of pairs of rare-earth elements." The results are given in table 1.

TABLE 1.—*Hydrothermal mineral syntheses*

Experiment	Constituents ¹	Temperature (degrees centigrade)	Duration (days)	Predominant phase identified
1.-----	$\text{CeCl}_3, \text{HCl}, \text{H}_3\text{PO}_4$ --	100 ± 3	5	Hexagonal CePO_4 .
2.-----	do-----	150 ± 3	5	Do.
3.-----	do-----	200 ± 3	5	Do.
4.-----	do-----	250 ± 10	5	Do.
5.-----	do-----	300 ± 10	5	Monazite.
6.-----	$\text{YCl}_3, \text{HCl}, \text{H}_3\text{PO}_4$ ---	300 ± 10	7	Xenotime.
7.-----	do-----	250 ± 10	3. 5	Do.
8.-----	do-----	200 ± 3	4	Do.
9.-----	do-----	150 ± 3	4	Do.
10.-----	do-----	105 ± 3	4	Do.
11.-----	do-----	50 ± 3	7	No precipitation.
(²)-----	do-----	85 ± 3	6	Do.
(³)-----	do-----	95 ± 3	7	Churchite.

¹ 0.1 g of oxide converted to chloride by evaporation to dryness with concentrated hydrochloric acid. The salts were dissolved in 2 ml of water containing 0.15 ml of concentrated hydrochloric acid. One ml of 2.1 percent (by volume) phosphoric acid was added with sufficient water to make a 4-ml volume.

² Solution, experiment 11, resealed and rerun.

³ Solution, experiment 11, again resealed and rerun.

An aqueous solution of cerous chloride and phosphoric acid, subjected to a temperature of 300°C and at approximately 90 atmospheres pressure for 5 days, produced monazite. Under the same conditions, yttrium chloride and phosphoric acid formed xenotime.

Attempts to synthesize monazite at temperatures between 100°C and 250°C were unsuccessful. The phosphates resulting at these lower temperatures gave X-ray powder diffraction patterns identical with a cerium phosphate described by Mooney (1950) as a "hexagonal modification." This was later found to be isostructural with the naturally occurring mineral rhabdophane, a hydrated cerium earth group phosphate (Palache and others, 1951, p. 774). A paper con-

cerning a reexamination of this mineral is in preparation by Hildebrand. Xenotime was synthesized at a considerably lower temperature than monazite. Xenotime formed at 105°C; at 95°C the resulting yttrium phosphate was found to be isostructural with the mineral churchite (weinschenkite, $\text{YPO}_4 \cdot 2\text{H}_2\text{O}$) (Palache and others, 1951, p. 771).

FRACTIONAL PHOSPHATE PRECIPITATION OF PAIRS OF RARE-EARTH ELEMENTS

METHODS OF PREPARATION

The rare earths used throughout these studies were of high purity, ranging between 99.0 and 99.8 percent. Ceric oxide was prepared by igniting primary-standard ammonium hexanitrate cerate obtained from G. Frederick Smith Chemical Co., Columbus, Ohio. Lanthanum, praseodymium, and neodymium oxides were obtained from The Institute for Atomic Research, Iowa State College, Ames, Iowa; samarium, ytterbium, and yttrium oxides from Research Chemicals, Inc., Burbank, Calif.; europium, gadolinium, terbium, dysprosium, holmium, erbium, thulium, and lutetium oxides from Johnson, Matthey Co., London.

The fractionation experiments of pairs of the rare-earth elements and the syntheses of the pure minerals described were done in much the same manner. Allowing for the higher oxidation state of CeO_2 , equal amounts of ignited oxides of the pairs were dissolved in hydrochloric acid in a small beaker. The amounts taken were 0.1 g each of the less costly oxides, such as those of La, Ce, Pr, Nd, Sm, and Y. For the more expensive oxides 0.020 g of each of Eu, Gd, Tb, Dy, Ho, Er, Tm, Yb, and Lu were taken. Hydrogen peroxide was added to those pairs that included cerium. For each pair the solution was evaporated to dryness, and the residue of rare-earth chlorides was dissolved in 2 ml of water containing 0.15 ml of concentrated hydrochloric acid. The solution was transferred to a silver crucible (15 ml true capacity). The beaker was rinsed twice with 0.5 ml of distilled water and the rinsings were added to the solution. One ml of 2.1 percent by volume phosphoric acid (1 ml of 0.8 percent by volume phosphoric acid for the smaller quantities taken) was added to the solution. These amounts of phosphoric acid were calculated to be enough to precipitate as phosphates one-fourth to one-half of the rare-earth elements present. The silver crucible was sealed with a thin silver disk and placed in a steel bomb (20 ml capacity) which contained 0.5 ml of water to counteract internal pressure. After heating at $300^\circ\text{C} \pm 10^\circ\text{C}$ for 5 days, the bomb was quickly cooled by cold running water. The silver seal was removed from the crucible and the fine crystalline phosphates in the solution

were filtered on a double filter paper, Whatman No. 42, and washed six times with distilled water acidified with hydrochloric acid. The filtrate was reserved. The phosphates were then sluiced from the filter paper with a fine jet of distilled water into a platinum dish. The suspension was evaporated to dryness on a steam bath and the dried phosphates were removed with a rubber policeman. Portions of the phosphates were examined by X-ray powder diffraction methods to determine the phases present and their relative unit-cell variations. Other portions were analyzed spectrographically to determine the ratios of the rare-earth pairs.

In the experiments on fractional precipitation, each reserved filtrate was treated with ammonium hydroxide in considerable excess to precipitate the rare earths in solution. Paper pulp was added and the solution was filtered after 1 hour through a Whatman No. 40 filter paper. The precipitate was washed 6 to 8 times with 5 percent ammonium hydroxide containing 2 percent ammonium chloride and then ignited at $1,000^{\circ}\text{C}$. These oxide fractions were also analyzed spectrographically to determine the rare earths present. In those experiments involving cerium, volumetric determinations of cerium in the recovered oxide fractions were also made. These analytical determinations permitted the calculation of separation factors. A chemical analysis of lanthanum phosphate that was produced in a bomb and was found to have the monazite structure by X-ray powder diffraction, showed the molecular ratio of La_2O_3 to P_2O_5 to be 1.00 to 0.97.

SEPARATION FACTORS

Evaluation of results of fractional precipitation processes have been expressed by various authors (Weaver, 1954a; Appleton and Selwood, 1941; Peppard and others, 1953) in terms of separation factors. These are empirical numerical values obtained by dividing the weight ratio of the elements in the precipitated fraction by the corresponding ratio in the unprecipitated fraction.

Our experiments confirmed the claim by Weaver that the separation factor is mathematically independent of the original ratio of a mixture of two elements as long as a constant fraction of the total is precipitated. Two experiments, in which the cerium to praseodymium starting ratios were 3 to 1 and 1 to 2, showed preferential precipitation of praseodymium to cerium in both, with identical separation factor values of 1.10. Two other experiments in which dysprosium to holmium starting ratios were 2 to 1 and 1 to 2, showed preferential precipitation of holmium to dysprosium in both instances, with identical separation factors of 1.20. The excellent agreement shown here is more fortuitous than real, because the analytical method used is accurate to only ± 2 percent. For the sake of uni-

formity, however, the weight ratio of each pair of the rare-earth oxides taken throughout our investigations was 1 to 1.

In the previous section on "Methods of preparation," it will be noted that the extent of precipitation of the phosphates of the more costly and of the less costly lanthanides varies by a ratio of 2 to 1. The purpose of the increased extent of precipitation of the more costly materials was to provide a sufficient yield of lanthanide phosphates for repeated spectrographic determinations. To ascertain the effect of this variation on the separation factor, cerium and lanthanum chlorides equivalent to 0.020 g each of their oxides were fractionated with 1 ml of 0.8 percent phosphoric acid. The separation factor was 1.46 as compared with 1.41 obtained in a previous fractionation of larger quantities of cerium and lanthanum using the smaller proportion of phosphoric acid. This variation in the separation factor is within experimental error and agrees with investigations by Weaver (1954a), who fractionated samarium-neodymium mixtures as oxalates and found only minor variations in separation factors between 17 percent and 56 percent precipitation.

SPECTROCHEMICAL DETERMINATIONS

PREPARATION OF STANDARDS

A series of standards was prepared from high-purity rare earths. Three standards were prepared for each rare-earth pair in the experiments on fractional precipitations by weighing exact quantities of each rare-earth oxide necessary to give weight ratios of 1.5, 1.0, and 0.67 of the heavier rare-earth oxide to the lighter rare-earth oxide. All the weight ratios of the oxides were based on trivalent rare earths, except for Pr and Tb which were calculated from Pr_2O_3 and Tb_2O_3 . The oxides were dissolved in a minimum amount of hydrochloric acid, precipitated with an excess of ammonium hydroxide, filtered, and ignited. The ignited oxides were then mixed with four parts of pure graphite.

APPARATUS AND OPERATING CONDITIONS

The apparatus and operating conditions used in this study are as follows:

Spectrograph.....	Grating spectrograph with Wadsworth mounting, dispersion 5.0 Å/mm.
Cathode.....	Graphite rod, 3-mm diameter.
Anode.....	Graphite, 6-mm diameter, cavity 4-mm deep, wall thickness 0.5 mm.
Samples and standards..	4 mg rare-earth oxides + 16 mg graphite, 6 mg rare-earth phosphates + 24 mg graphite. The sample weight is 1.5 times greater for the phosphates than for the oxides because of the lower content of the rare-earth elements in the phosphates.

Analytical gap.....	3 mm, maintained throughout excitation period.
Excitation source.....	250 v ballasted d-c arc, 16 amp.
Length of exposure.....	Samples arced to completion.
Emulsion.....	Eastman type III-0, developed 21° C in DK-50 for 5 minutes with continuous agitation.
Wave-length region....	2300-3500Å.
Microphotometer.....	Projection comparator-microphotometer using a scanning slit at the plate.
Emulsion calibration---	Iron line group method of Dieke and Crosswhite (1943).
Exposure index.....	Fe 3157.88 Å, transmitting 25 percent in an iron arc exposed for 120 seconds at 5.5 amp.

A 2-step filter transmitting nominally 50 and 100 percent of the light was placed at the slit to obtain spectra at 2 different densities. The arc image was focused on the slit at 5.5 magnification, and the light from the central 4-mm portion was allowed to enter the slit of the spectrograph.

LINE PAIRS

Most of the spectrochemical methods for the determination of rare earths have been developed in recent years to test the purity of the different rare-earth fractions obtained in purification processes (Fassel and others, 1952, 1955; Fassel and Wilhelm, 1948; Norris and Pepper, 1952) or to analyze total rare earths which have been chemically concentrated from rocks and minerals (Rose and others, 1954; Waring and Mela, 1953). Methods of both categories in general require the use of the more sensitive analytical lines of the individual rare-earth elements. The analytical lines used in this study were of much weaker intensity because the determined elements were present in major amounts.

Spectrographic determinations were made on both the fractionally precipitated phosphates and the rare earths which remained in solution. As discussed previously, the rare earths were recovered from the filtrate and ignited to the oxides. The weight ratios of the rare-earth oxides in the phosphate precipitates and oxides from filtrates were expected to fall above and below the 1.0 weight ratio standard on the analytical curve. The most important consideration in the choice of line pairs was to select a line pair in the 1.0 weight ratio standard so that the intensity ratio would be near unity. Many line pairs were investigated to find lines close together which would meet this requirement. The use of a 2-step filter proved to be invaluable since it provided 2 different densities for each line and 4 combinations of intensity ratios for each line pair.

The spectra of many of the rare-earth elements are extremely complex and their term analysis has been found to be unusually difficult. The term classification data (Albertson and Harrison, 1937; King, 1928, 1933, 1935, 1939, 1941; Meggers, 1928; Meggers and Scribner,

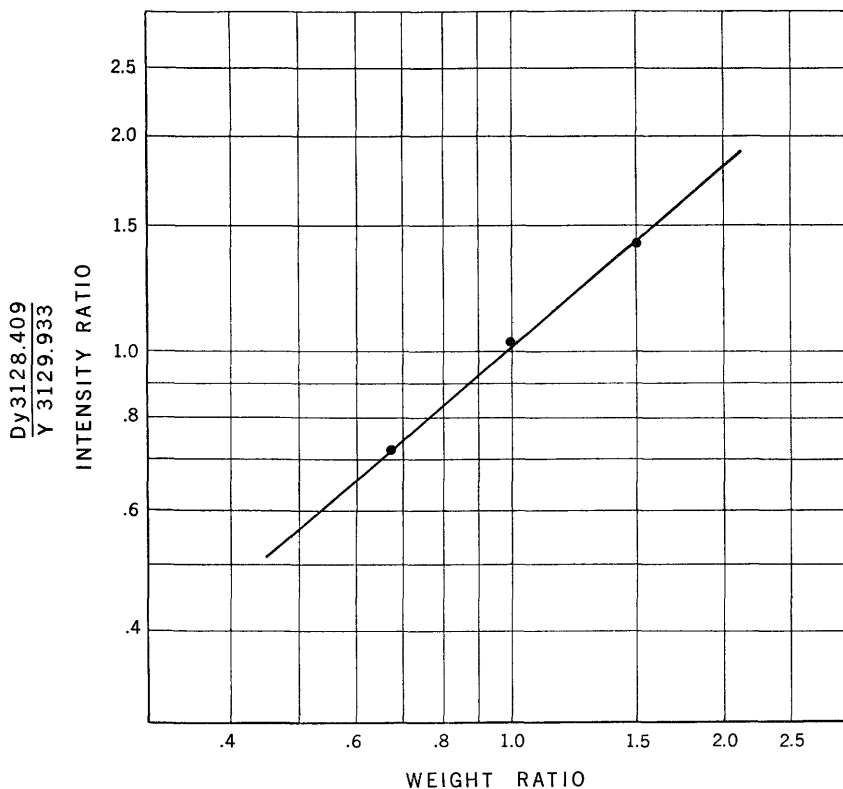


FIGURE 44.—A typical working curve of the rare-earth pairs.

1937a, 1937b; Russell, 1950) are incomplete and no information is available for some of the analytical lines used. Wherever possible, lines of the singly ionized ion were selected. The line pairs used in this study are given in table 2. The table includes the intensity ratios of the standards which could be useful in any future study of the fractional precipitation of rare-earth pairs. The analytical curves for the line pairs are very similar, differing only slightly in their slopes. The Dy 3128.409:Y 3129.933 line pair is shown in figure 44 and represents a typical working curve.

The weight ratio of the oxides in Ce:Y phosphate could not be determined directly because the precipitate proved to be extremely high in Y and low in Ce. The weight ratio of the oxides in the Ce:Y oxides was found to be 1.75, and the weight ratio of the oxides in the phosphates was calculated to be 0.07.

TABLE 2.—*Rare-earth line pairs and the intensity ratios of the standards*

Line pair	Intensity ratios as oxides of the standards			Line pair	Intensity ratios as oxides of the standards		
	1.50	1.00	0.67		1.50	1.00	0.67
Ce II 3056.777	1.49	1.08	0.77	Er 2765.617	1.29	1.0	0.75
La II 3104.589				Ho 2766.85			
Ce I 2874.551	1.32	.92	.65	Er 2581.582	1.22	.97	.76
La II 2893.071				Ho 2610.51			
Pr II 3121.571	1.26	.93	.67	Tm 3210.820	1.26	.94	.74
Ce II 3155.793				Er 3205.148			
Pr II 3163.735	1.69	1.28	.93	Tm 2660.090	1.11	.87	.70
Ce II 3154.506				Er 2672.246			
Nd II 3141.476	1.65	1.24	.91	Yb II 2718.340	1.35	1.04	.84
Pr II 3121.571				Tm 2742.960			
Nd II 3133.603	1.20	.92	.73	Yb II 3080.110	1.20	.90	.69
Pr II 3168.242				Tm 2650.270			
Sm II 3136.297	1.21	.88	.63	Lu II 3027.290	1.30	.96	.66
Nd II 3141.476				Yb II 3026.668			
Sm II 3136.297	1.40	1.10	.88	Lu I 3080.110	1.20	1.04	.71
Nd II 3134.897				Yb II 3098.879			
Eu II 3054.930	1.31	.95	.67	Sm II 3136.297	1.48	1.05	.77
Sm II 3136.297				Y II 3086.858			
Eu II 3077.353	1.36	1.02	.75	Sm II 3117.725	1.29	.96	.72
Sm II 3046.933				Y I 3114.283			
Gd II 3089.957	1.21	.89	.63	Gd II 3108.364	1.25	.95	.72
Eu II 3054.930				Y II 3112.032			
Gd II 3282.257	1.46	.99	.68	Gd II 3040.340	1.72	1.24	.91
Eu II 3278.54				Y I 3045.369			
Tb 2956.210	1.17	.90	.70	Eu I 2991.340	1.60	.95	.69
Gd II 2923.371				Y II 2984.256			
Tb 3135.350	1.22	.96	.76	Eu II 3960.230	1.56	.95	.66
Gd II 3098.903				Y I 2964.968			
Dy 2913.952	1.21	.93	.73	Dy 2985.930	1.30	.94	.72
Tb 2916.260				Y I 2984.256			
Dy 2948.323	1.17	.91	.69	Dy 3128.409	1.34	1.07	.77
Tb 2956.210				Y II 3129.933			
Ho 2610.51	1.24	.98	.79	Yb II 3117.804	1.28	.96	.62
Dy 2634.811				Y II 3129.933			
Ho 3038.690	1.47	1.16	.90	Yb II 2983.980	1.20	.88	.62
Dy 3043.144				Y I 2984.256			

PRECISION AND ACCURACY

The data on the precision of the method are shown in table 3. The coefficient of variation for a single determination is about 2 percent as calculated from two of the synthetic unknowns exposed in duplicate on different plates on different days over a period of several months.

TABLE 3.—*Precision of spectrochemical determination*

Rare-earth pair	Average weight ratio	Number of determinations	Coefficient of variation
Sm:Nd.....	1.36	6	2.1
Tb:Gd.....	.90	6	1.7

The coefficient of variation ν is calculated as follows:

$$\nu = \frac{100}{C} \sqrt{\frac{d^2}{n-1}}$$

C is the average weight ratio,

d is the difference of the determination from the mean,

n is the number of determinations.

The accuracy of the method was tested by analyzing synthetic unknowns prepared in the same way as the standards. The results of the tests are given in table 4. The maximum percentage deviation from the true value amounted to 3 percent in the determination of the Yb:Tm weight ratio. Only two of the rare-earth pairs studied by the spectrochemical method were tested by an independent method. Cerium was determined volumetrically in the Ce:La and Pr:Ce oxide fractions, and the weight ratios compared with those obtained spectrochemically. The volumetrically determined value for Ce:La was 0.83, and the spectrochemical value, 0.85. The volumetrically determined value for Pr:Ce was 0.93, and the spectrochemical value, 0.95. The agreement between the two methods is good and suggests that the accuracy of the spectrochemical determinations is equal to the precision.

The results of the spectrochemical analyses of all adjacent pairs are given in table 5.

TABLE 4.—*Analyses of synthetic unknowns*

Rare-earth pair (as oxides)	Spectrochemical analysis (oxide ratio)	True value (oxide ratio)
Ce:La.....	0.71	0.71
Sm:Nd.....	1.36	1.33
Eu:Sm.....	.76	.75
Tb:Gd.....	.90	.90
Dy:Tb.....	1.12	1.11
Yb:Tm.....	1.37	1.33
Gd:Y.....	.82	.80

TABLE 5.—*Spectrochemical analyses and phases produced from fractionally precipitated lanthanide phosphate pairs*

Lanthanide pair ¹	Average ionic radius ²	Ratio in phosphate precipitate ³	Ratio in filtrate ³	Separation factor	Phases produced ⁴
Ce:La-----	1. 20 { La 1. 22 Ce 1. 18 }	1. 20	0. 85	1. 41	M
Pr:Ce-----	1. 17 { Ce 1. 18 Pr 1. 16 }	1. 08	. 95	1. 14	M
Nd:Pr-----	1. 155 { Pr 1. 16 Nd 1. 15 }	1. 11	. 92	1. 21	M
Sm:Nd-----	1. 14 { Nd 1. 15 Sm 1. 13 }	1. 06	. 90	1. 18	M
Eu:Sm-----	1. 125 { Sm 1. 13 Eu 1. 12 }	. 93	1. 06	. 88	M
Gd:Eu-----	1. 115 { Eu 1. 12 Gd 1. 11 }	. 82	1. 15	. 71	M
Tb:Gd-----	1. 10 { Gd 1. 11 Tb 1. 09 }	1. 10	. 93	1. 18	M, x
Dy:Tb-----	1. 08 { Tb 1. 09 Dy 1. 07 }	1. 10	. 94	1. 17	X, m
Ho:Dy-----	1. 06 { Dy 1. 07 Ho 1. 05 }	1. 10	. 90	1. 22	X
Er:Ho-----	1. 04 { Ho 1. 05 Er 1. 03 }	1. 13	. 83	1. 36	X
Tm:Er-----	1. 02 { Er 1. 03 Tm 1. 01 }	1. 16	. 80	1. 45	X
Yb:Tm-----	1. 005 { Tm 1. 01 Yb 1. 00 }	1. 13	. 79	1. 43	X
Lu:Yb-----	0. 995 { Yb 1. 00 Lu 0. 99 }	. 91	1. 07	. 85	X

¹ Original oxide ratio is 1.00.² Individual values of ionic radii from Goldschmidt (1954).³ Weight ratio of the heavier lanthanide oxide to the lighter lanthanide oxide.⁴ M=monazite, X=xenotime. m=monazite in minor amount. x=xenotime in minor amount.

X-RAY DETERMINATIONS

For each of the synthesized lanthanide pairs, a powder diffraction pattern was prepared to determine the number and kind of phases present as well as to observe by visual comparison the progressive contraction of the unit cells from LaPO_4 to LuPO_4 in accordance with the concept of the lanthanide contraction (Goldschmidt and others, 1925). The interplanar spacing data for each pattern are shown in table 6. The X-ray powder data for LaPO_4 and LuPO_4 (cols. 1 and 20, respectively) have been inserted in table 6 only to show that they have the largest and smallest unit cells of all the lanthanides. YPO_4 (col. 15) has been inserted to show its relative position with respect to the other compounds. Natural monazite from Magnet Cove, Ark. (col. 4), and natural xenotime from the Shelby quadrangle, N. C. (col. 14), have been inserted to show the relative positions of these minerals in the series. Powder patterns of other natural monazites and xenotimes were found to vary but little from the data shown in columns 4 and 14.

TABLE 6.—X-ray powder diffraction data for synthetic and natural rare-earth phosphates

Monazite structure									
1	2	3	4	5	6	7	8	9	10
	(Ce _{0.9} La _{0.1}) PO ₄ Film 8280	(Pr _{0.95} Ce _{0.05}) PO ₄ Film 8352	Monazite Film 8698	(Nd _{0.95} Pr _{0.05}) PO ₄ Film 8653	(Sm _{0.95} Nd _{0.05}) PO ₄ Film 8483	(Eu _{0.95} Sm _{0.05}) PO ₄ Film 8505	(Gd _{0.95} Eu _{0.05}) PO ₄ Film 8531	(Tb _{0.95} Gd _{0.05}) PO ₄ Film 8532	(Dy _{0.95} Tb _{0.05}) PO ₄ Film 8593
$d(\text{\AA})$, meas.)	$d(\text{\AA})$, meas.)	$d(\text{\AA})$, meas.)	$d(\text{\AA})$, meas.)	$d(\text{\AA})$, meas.)	$d(\text{\AA})$, meas.)	$d(\text{\AA})$, meas.)	$d(\text{\AA})$, meas.)	$d(\text{\AA})$, meas.)	$d(\text{\AA})$, meas.)
I	I	I	I	I	I	I	I	I	I
5.22	5.21	5.20	5.20	5.17	5.16	5.14	5.13	5.10	
4.83	4.82	4.80	4.82	4.78	4.75	4.72	4.70	4.67	101
4.70	4.67	4.66	4.66	4.65	4.62	4.58	4.56	4.55	110
4.19	4.18	4.17	4.17	4.15	4.13	4.12	4.11	4.06	011
4.10	4.10	4.08	4.08	4.08	4.04	4.01	3.99	3.97	111
3.53	3.52	3.51	3.51	3.48	3.47	3.44	3.43	3.41	111
3.31	3.30	3.29	3.30	3.28	3.25	3.23	3.22	3.20	200
3.12	3.11	3.10	3.10	3.09	3.06	3.04	3.02	3.01	210
3.01	3.00	2.98	2.99	2.98	2.94	2.92	2.91	2.91	210
2.88	2.88	2.87	2.87	2.86	2.82	2.81	2.81	2.81	112, 012
2.61	2.61	2.61	2.61	2.59	2.57	2.55	2.56	2.56	202
2.45	2.44	2.44	2.44	2.43	2.40	2.40	2.39	2.39	211
2.42	2.40	2.40	2.40	2.39	2.37	2.36	2.35	2.34	212, 112
2.35			2.34						
2.26			2.25						
2.21	2.20	2.19	2.19	2.18	2.16	2.15	2.14	2.14	
2.15	2.15	2.14	2.15	2.13	2.12	2.11	2.10	2.09	
2.13	2.13	2.13	2.13	2.11	2.10	2.09	2.08	2.07	
2.04			2.02						
1.981	1.973	1.961	1.961	1.957	1.941	1.926	1.918	1.910	
		1.957	1.933	1.929	1.910	1.903	1.895	1.884	
1.914	1.903	1.895	1.895	1.888	1.873	1.870	1.859	1.852	
	1.877	1.866	1.870	1.866	1.855	1.845	1.838	1.831	
1.884	1.870	1.859	1.859	1.852	1.841	1.834	1.824	1.813	
			1.797						
1.817	1.768	1.759	1.762	1.755	1.749	1.734	1.731	1.728	
1.774	1.746	1.740	1.737	1.731	1.719	1.707	1.698	1.695	
1.755	1.701	1.692	1.689	1.687	1.678	1.664	1.658	1.647	
1.707	1.655	1.647	1.645	1.639	1.631	1.621	1.610	1.610	
1.672	1.629	1.623	1.623	1.618	1.610	1.600	1.598	1.593	
1.634	1.610	1.605	1.600	1.598	1.588	1.578	1.578	1.563	
1.616	1.549	1.549	1.549	1.542	1.530	1.520	1.508	1.503	
1.558	1.540	1.538	1.535	1.519	1.517	1.512	1.447	1.443	
1.544	1.471	1.465	1.463	1.459	1.451	1.447	1.425	1.423	
1.480				1.447	1.439				

1.400	4	1.393	1.386	1.423	2	1.380	1.370	1.363	1.358	1.354
1.372	3	1.377	1.372	1.366	3	1.366	1.358	1.347	1.344	1.339
1.352	11	1.346	1.336	1.339	9	1.331	1.323	1.313	1.307	1.301
1.339	6	1.332	1.329	1.329	9	1.323	}			
				1.307	2					
				1.280	9					
1.259	4	1.238	1.226	1.201	9	1.229	1.221	1.212	1.209	1.204
1.244	?(AgCl)			1.183	9					
				1.168	6					
1.169	6	1.162	1.158	1.153	3	1.152	1.144	1.136	1.133	1.128
1.159	7	1.154	1.149	1.145	2	1.145	1.138	1.129	1.127	1.121
				1.121	4					
1.097	6	1.092	1.087	1.099	4	1.082	1.074	1.069	1.065	1.060
				1.086	2					
				1.074	2					
1.055	4	1.051	1.045	1.064	3	1.041	1.035	1.027	1.026	1.021
				1.046	4					
				1.034	2					
				1.025	2					
				1.014	2					
				1.008	2					
				.9899	2					
				.9659	2					
				.8523	3					
.9457	4	.9388	.9348	.9343	3	.9304	.9250	.9181	.9161	.9120
				.9181	3					
				.9012	3					
				.8831	3					
				.8667	3					
				.8462	3					
				.8320	3					
				.8238	3					
				.8134	2					
				.8038	2					
				.7966	3					

.9621	.9694 _{α1}	.9576 _{α1}	2	.9557 _{α1}	2	.9533 _{α1}	.9521 _{α1}	.9702 _{α1}	.9657 _{α1}	5
.9641	.9497 _{α1}	.9491 _{α1}	2	.9461 _{α1}	2	.9449 _{α1}	.9438 _{α1}	.9473 _{α1}	.9652 _{α1}	2
.9332	.9313 _{α1}	.9291 _{α1}	4	.9118 _{α1}	5	.9103 _{α1}	.9088 _{α1}	.9195 _{α1}	.9420 _{α1}	4
.9197	.9153 _{α1}	.9138 _{α1}	2	.8828 _{α1}	4	.8815 _{α1}	.8794 _{α1}	.9058 _{α1}	.9358 _{α1}	6
.8890 _{α1}	.8863 _{α1}	.8846 _{α1}	2	.8672 _{α1}	4	.8645 _{α1}	.8639 _{α1}	.8756 _{α1}	.9226 _{α1}	2
.8720 _{α1}	.8690 _{α1}	.8680 _{α1}	2	.8541 _{α1}	1	.8539 _{α1}	.8523 _{α1}	.8696 _{α1}	.9148 _{α1}	20
.8656 _{α1}	.8655 _{α1}	.8655 _{α1}	.7	.8465 _{α1}	.9	.8451 _{α1}	.8423 _{α1}	.8546 _{α1}	.9024 _{α1}	25
.8516 _{α1}	.8478 _{α1}	.8471 _{α1}	.5	.8371 _{α1}	1	.8365 _{α1}	.8350 _{α1}	.8482 _{α1}	.8867 _{α1}	4
.8402 _{α1}	.8371 _{α1}	.8371 _{α1}	1	.8294 _{α1}	.7	.8294 _{α1}	.8284 _{α1}	.8327 _{α1}	.8724 _{α1}	13
	.8310 _{α1}	.8305 _{α1}	.7	.8120 _{α1}	.9	.8050 _{α1}	.8031 _{α1}	.8058 _{α1}	.8664 _{α1}	5
.8106 _{α1}	.8085 _{α1}	.8074 _{α1}	4	.8061 _{α1}	5			.8001 _{α1}	.8607 _{α1}	2
	.7870 _{α1}	.7876 _{α1}	.3	.7863 _{α1}	.9			.7982 _{α1}	.8552 _{α1}	11
.7768 _{α1}	.7768 _{α1}	.7755 _{α1}	.1	.7843 _{α1}	2			.7781 _{α1}	.8492 _{α1}	2
								.7760 _{α1}	.8448 _{α1}	9
									.8401 _{α1}	2
									.8374 _{α1}	9
									.8267 _{α1}	6
									.8242 _{α1}	4
									.8220 _{α1}	9
									.8154 _{α1}	3
									.8011 _{α1}	4
									.7985 _{α1}	25
									.7925 _{α1}	4
									.7886 _{α1}	4
									.7760 _{α1}	9

1 Weight ratios of the elements calculated from the weight ratios of the oxides in the phosphate precipitates listed in table 5. Accuracy of the weight ratios of the elements is ± 3 percent.

From A. Pakst, Am. Min. v. 36, no. 1-2, 1951, p. 63.

From Am. Soc. Testing Materials. Card 5-0454.

The diffraction patterns were taken with Debye-Scherrer powder cameras (114.59 mm diameter) using the Straumanis technique with $\text{CuK}\alpha$ (Ni filter), $\lambda=1.5418$ A. λ for $\text{K}\alpha_1=1.5405$. The cut-off point for these cameras is at a 2θ value of approximately 5° . Measurements were made with a Hilger-Watts film-measuring rule with a vernier precision of 0.05 mm. Shrinkage corrections were determined and appropriately applied to each film. Intensities were measured with calibrated film strips prepared such that successive step exposures are related to each other by a factor of $\sqrt{2}$. Intensity values were not measured for all the synthetic products because many of them showed the effects of preferred orientation. Because the intensity relationships are not pertinent to the problem at hand, no attempts were made to eliminate the preferred orientation condition. Most of the synthetic products contained a moderate to large amount of AgCl and a small amount of Ag (contaminants from the silver crucible), but these phases were readily recognizable and did not conflict with interpretation and measurement of the powder patterns.

RESULTS

In table 5 are given spectrochemical results and phases produced in all the fractionation experiments of adjacent pairs of the entire suite of lanthanides. Separation factors were calculated for each lanthanide pair. Also shown are average ionic radii of the pairs, which are simple arithmetic means of values as given by Goldschmidt (1954, p. 89). The fractionation experiments indicate that the lanthanide phosphates obtained by this procedure form monazite, xenotime, or mixtures of both phases and that fractional precipitation in this system is a preferential process. Of those lanthanides that form monazite only, the heavier ones precipitated in preference to the lighter ones. A reversal occurred with the Eu, Sm pair, where the lighter lanthanide, Sm , precipitated preferentially to the heavier, Eu . This reversal continued through the Gd, Eu pair. With Tb, Gd the order of preferential precipitation reverted to the heavier lanthanide, Tb , and a mixture of xenotime and monazite appeared, with monazite predominating. At Dy, Tb the heavier lanthanide, Dy , precipitated preferentially to Tb and again a mixture of xenotime and monazite appeared, but with the xenotime phase predominating. At Ho, Dy all evidence of the monazite phase disappeared. Preferential precipitation continued to favor the heavier lanthanide of the pairs until the Lu, Yb pair where another reversal is evident.

The X-ray diffraction data in table 6 show that the monazite phase was produced in each pair from $(\text{Ce, La})\text{PO}_4$ (col. 2) through $(\text{Dy, Tb})\text{PO}_4$ (col. 10), whereas the xenotime phase was produced in pairs from $(\text{Tb, Gd})\text{PO}_4$ (col. 11) through $(\text{Lu, Yb})\text{PO}_4$ (col. 20). In

the pairs (Tb,Gd)PO₄ and (Dy,Tb)PO₄ (cols. 9, 10, 11, and 12) in the transition zone, both of these phases were present (table 5) so that the pairs in columns 9 and 10 showing the data for the monazite phase were repeated in columns 11 and 12 to show the data for the xenotime phase. In this transition zone the Tb,Gd pair consisted predominantly of the monazite phase with a small amount of the xenotime phase whereas the adjacent Dy,Tb pair consisted predominantly of the xenotime phase with a small amount of the monazite phase.

To determine more precisely the transition point between the cerium subgroup with the monazite structure and the yttrium subgroup with the xenotime structure, bomb preparations of the single rare-earth phosphates of Sm, Eu, Gd, Tb, Dy, and Y were made (table 7). X-ray examinations of these show that SmPO₄ (bomb 32), EuPO₄ (bomb 26), and GdPO₄ (bombs 27 and 38) have the monazite structure and TbPO₄ (bomb 31), DyPO₄ (bombs 34 and 78) and YPO₄ (bomb 30) have the xenotime structure. With particular reference to TbPO₄ produced in glass ampoules (bombs 28 and 56), the ampoules broke during the experiments, but the recovered products, which included bits of glass and perhaps iron chloride, were found by X-ray examination to have the monazite structure. This demonstrates that TbPO₄ may be dimorphic because it acquired the xenotime structure when prepared in silver crucibles and the monazite structure when prepared in glass ampoules. This also establishes the transition point in the lanthanide series at TbPO₄.

TABLE 7.—*Hydrothermal syntheses of some single rare-earth phosphates*

Bomb	Rare-earth oxide ¹	Weight of oxide taken (gram)	Type of container	Predominant phase produced
32	Sm ₂ O ₃	0.027-----	Silver crucible---	Monazite.
26	Eu ₂ O ₃	.015-----	Glass ampoule--	Do.
27	Gd ₂ O ₃	.015-----	do-----	Do.
38	Gd ₂ O ₃	.028-----	Silver crucible---	Do.
28	Tb ₄ O ₇	.012-----	Glass ampoule--	Do.
31	Tb ₄ O ₇	.017-----	Silver crucible---	Xenotime.
56	Tb ₄ O ₇	.015-----	Glass ampoule---	Monazite.
34	Dy ₂ O ₃	.019-----	Silver crucible---	Xenotime.
78	Dy ₂ O ₃	.025(+ 0.2g SiO ₂)---	do-----	Do.
30	Y ₂ O ₃	.02-----	do-----	Do.

¹ Each oxide was converted to chloride by evaporation to dryness with concentrated hydrochloric acid. The salts were taken up in 2 ml of water containing 0.15 ml of concentrated hydrochloric acid. One ml of 0.8 percent (by volume) phosphoric acid was added with sufficient water to make a 4-ml volume. Each was heated at 300°C. ± 10°C, 90 atmospheres pressure, for 5 days.

The relation of yttrium phosphate to the lanthanide phosphates can be seen from the results of fractionation experiments given in table 8. It may be assumed that yttrium will precipitate preferentially to all the lanthanides of the cerium subgroup because it was shown that

yttrium is precipitated preferentially to dysprosium of the yttrium subgroup. This assumption is further justified by the fact that in the experiment with the Ce,Y pair, the solid phase was sufficiently enriched in yttrium, so that no evidence of a monazite phase was detected. In the experiments with the Sm,Y and the Eu,Y pairs, there was evidence of the monazite phase, but the weight ratios indicate predominance of the xenotime phase in both pairs. It might be expected that the experiment with the Gd,Y pair would also show two phases, but only the xenotime phase was detected. Ytterbium was found to precipitate preferentially to yttrium, thus placing yttrium in the phosphate system between dysprosium and ytterbium. Comparison of the relative unit-cell sizes from X-ray powder diffraction patterns more definitely established the position of yttrium phosphate at the Er,Ho pair. Assuming that only the xenotime phase would be present, X-ray powder diffraction patterns were not made of the Dy,Y and Yb,Y pairs.

TABLE 8.—*Spectrochemical analyses of fractionally precipitated yttrium and some lanthanide phosphates*

[Heated at 300°C for 5 days]

Lanthanide and yttrium pairs	Ratio in phosphate precipitate ¹	Ratio in filtrate ¹	Separation factor	Phases present ²
Ce:Y ³ -----	⁴ 0. 07	1. 75	0. 04	X
Sm:Y ³ -----	. 56	1. 30	. 43	X + M
Eu:Y ⁵ -----	. 82	1. 33	. 62	X + M
Gd:Y ⁶ -----	. 60	1. 35	. 44	X
Dy:Y ⁵ -----	. 80	1. 15	. 70	-----
Yb:Y ⁵ -----	1. 60	. 67	2. 39	-----

¹ Weight lanthanide oxide:weight yttrium oxide.

² X=xenotime, M=monazite.

³ 0.1 gram of each oxide was converted to chlorides, dissolved in 3 ml of water containing 0.15 ml of concentrated hydrochloric acid, and then 1 ml of 2.1 percent (by volume) phosphoric acid was added.

⁴ Calculated from the oxide ratio in the filtrate.

⁵ 0.02 gram of each oxide was treated as in footnote 3 except that 1 ml of 0.8 percent (by volume) phosphoric acid was added.

⁶ 0.05 gram of each oxide was treated as in footnote 3.

DISCUSSION OF RESULTS

In fractional precipitation studies, preferential precipitations indicate the relative solubility of analogous compounds of two or more elements. The compounds of the lanthanide elements are ideal for such studies inasmuch as they form an extended series containing elements closely related structurally and chemically. In this investigation the heavier lanthanide of the pairs exhibited greater insolubility, reaching maximum insolubility at samarium in the cerium subgroup and at ytterbium in the yttrium subgroup. While the greater insolubility of the heavier lanthanide may be explained,

in part, as a function of decreasing ionic radius, the reversals in solubility shown with Eu, Gd, and Lu offer contradictory evidence to this concept. The need for a more adequate explanation of these reversals is apparent. It is noteworthy that in the transition zone from the monazite structure to the xenotime structure two phases were observed in the X-ray patterns. Under the microscope these two-phase products were observed to have a needlelike habit; no other morphological forms could be observed. The Tb,Gd pair, which was predominantly monazite, and the adjacent Dy,Tb pair, which was predominantly xenotime, formed these needlelike crystals. The other adjacent pair, Eu,Sm, which was all monazite, showed an irregular shape characteristic of all other lanthanide pairs.

Reversals in most systems involving the lanthanides appear to be the rule rather than the exception. Except for the dimethyl phosphate system at 25°C in which the solubility of the lanthanides falls steadily from lanthanum to ytterbium, the lanthanide salts generally show reversals (Yost and others, 1947). In the oxalate system (Weaver, 1954c) the solubility decreases to a minimum at samarium, followed by increasing solubility that persists through ytterbium. The systems $R_2(SO_4)_3 \cdot 8H_2O$ at 20°C and $R(BrO_3)_3 \cdot 9H_2O$, where R is the individual lanthanide or yttrium, also show decreasing solubilities of the lanthanides from praseodymium and lanthanum to europium and gadolinium, respectively (Yost and others, 1947), followed by increasing solubilities that continue through lutetium and terbium.

The variation of separation factor values of the heavier to the lighter of each lanthanide pair is shown in figure 45. Preferential precipitation of the heavier to the lighter lanthanide is indicated by a separation factor greater than 1.00. Values less than 1.00, as shown by the Sm,Eu and Yb,Lu pairs, indicate 2 reversals in solubilities with maximum insolubilities at samarium and ytterbium, respectively. The Eu,Gd pair, for which the value is also less than 1.00, is interpreted as a continuation of the reversal at the Sm,Eu pair. Experimental studies now in progress indicate that these data may be used for predicting preferential precipitations of widely separated pairs. Details will be published later.

The position of yttrium in the lanthanide series has been variously reported in different studies (Kettelle and Boyd, 1947; Vickery, 1953; Weaver, 1954b) to be between Tb and Tm. X-ray diffraction patterns provide an excellent means for measuring the lanthanide contraction (Goldschmidt and others, 1925). This is a unique property of the series, related to continual diminishing size of the ionic radii of the lanthanides. In the phosphate system each successive pair of adjacent lanthanides showed smaller unit cells as the mean ionic radius of the pair decreased. From the powder data it can be seen that yttrium

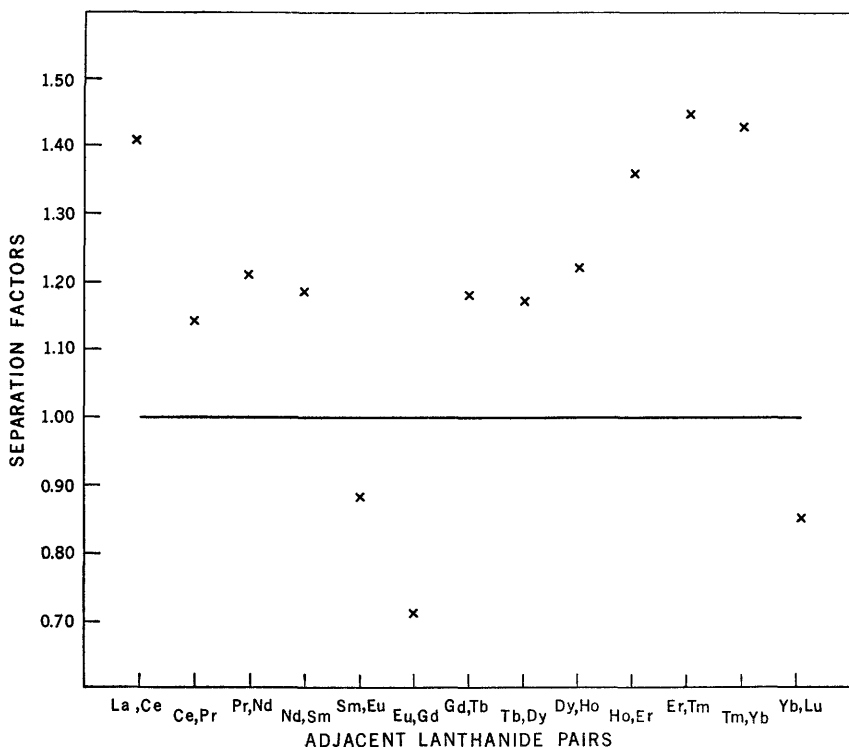


FIGURE 45.—Variation of separation factors.

$$\text{Separation factor} = \frac{\frac{\text{Weight of heavier lanthanide oxide}}{\text{Weight of lighter lanthanide oxide}} \text{ in precipitate}}{\frac{\text{Weight of heavier lanthanide oxide}}{\text{Weight of lighter lanthanide oxide}} \text{ in filtrate}}$$

phosphate has unit-cell dimensions very close to that of the Ho,Er pair.

Our experiments have shown that at moderate temperature (300°C) and pressure (approximately 90 atmospheres) yttrium phosphate precipitates preferentially to all the cerium subgroup lanthanides. Hence, from solutions containing yttrium and all other lanthanides, initial precipitates should tend to be rich in yttrium. With regard to mineralogical significance this finding is supporting evidence for judging the sequence of crystallization and deposition of the natural minerals. Bjørlykke (1935) postulated simultaneous crystallization of monazite and xenotime. Assuming that the natural process is one of fractionation under conditions of moderate temperatures and pressures, then,

as yttrium forms xenotime, our experiments indicate that xenotime would fractionally crystallize first. Yttrium and the lanthanides of its subgroup would be expected to combine first with any phosphorus present, coprecipitating only minor amounts of the cerium subgroup lanthanides. Additional phosphorus would then lead to the formation of monazite with a major quantity of the cerium subgroup lanthanides. However, taking into account the complex systems from which minerals form in nature, the possibility of prior deposition of monazite cannot be precluded. Future crystallization studies of systems more complex than the simple one presented here may indicate such order of deposition.

Of special interest regarding the hexagonal cerium phosphate produced between 100°C and 250°C and the natural occurring mineral rhabdophane are the results of three experiments. Solutions containing cerium chloride, phosphoric and hydrochloric acids, in the amounts used in the silver crucible syntheses, were sealed in Pyrex test tubes and kept immersed in a steam bath (approximately 97°C) for 5 days, 4 months, and 1 year, respectively. The phosphates from the first two experiments gave X-ray powder diffraction patterns isostructural with hexagonal cerium phosphate and rhabdophane. The phosphates that remained for 1 year were isostructural with monazite (monoclinic), confirming Mooney's (1950) claim that long digestion periods tend to cause conversion to the monoclinic form. These experiments demonstrated that a phosphate isostructural with monazite can be produced at a much lower temperature and pressure if given sufficient time.

In other experiments, natural occurring rhabdophane from Salisbury, Conn. (Palache and others, 1951, p. 774), was converted to monazite, and churchite, described as weinschenkite from the Kelly Bank mine, Vesuvius, Va. (Milton and others, 1944), was converted to xenotime by sealing the minerals in silver crucibles containing 4 ml of water and heating at 300°C for 5 days. The radial fibrous crystal habit of both rhabdophane and churchite was maintained in these experiments, showing that pseudomorphism of monazite and xenotime may be possible in the natural minerals, although such evidence of pseudomorphism has not been observed in nature.

It seems from these experiments that both rhabdophane and churchite are less stable than monazite and xenotime, respectively. Therefore, it is not unlikely that some present monazite and xenotime samples were precipitated initially as rhabdophane or churchite.

LITERATURE CITED

- Albertson, W. E., and Harrison, G. R., 1937, Preliminary analysis of the first spark spectrum of cerium, Ce II: *Phys. Rev.*, v. 52, p. 1209-1215.
- Appleton, D. B., and Selwood, P. W., 1941, Fractional partition of the rare earths: *Am. Chem. Soc. Jour.*, v. 63, p. 2029.
- Børlykke, Harald, 1935, The mineral paragenesis and classification of the granite pegmatites of Iveland, Setesdal, Southern Norway: *Norsk. Geol. Tidsskr.*, v. 14, p. 211-309.
- Dieke, G. H., and Crosswhite, H. M., 1943, The use of iron lines as intensity standards: *Optical Soc. America Jour.*, v. 33, no. 8, p. 425-434.
- Fassel, V. A., Cook, H. D., Krotz, L. C., and Kehres, P. W., 1952, Quantitative spectrographic analysis of the rare-earth elements. IV. Determination of cerium, praseodymium, and neodymium in lanthanum, V. Determination of lanthanum, praseodymium, and neodymium in cerium, VI. Determination of lanthanum, cerium, and neodymium in praseodymium, VII. Determination of praseodymium in neodymium: *Spectrochimica Acta*, v. 5, p. 201-209.
- Fassel, V. A., Quinney, Beverly, Krotz, L. C., and Lentz, C. F., 1955, Quantitative spectrographic analysis of rare-earth elements. Determination of holmium, erbium, yttrium, and terbium in dysprosium, Determination of yttrium, dysprosium, and erbium in holmium, and Determination of yttrium, dysprosium, holmium, thulium, and ytterbium in erbium: *Anal. Chemistry*, v. 27, p. 1010-1014.
- Fassel, V. A., and Wilhelm, H. A., 1948, Quantitative spectrographic analysis of the rare-earth elements. I. Determination of samarium in neodymium, II. Determination of europium in samarium: *Optical Soc. America Jour.*, v. 38, p. 518-526.
- Goldschmidt, V. M., 1954, *Geochemistry*, London, Oxford Univ. Press, p. 730.
- Goldschmidt, V. M., Barth, Tom, and Lunde, G., 1925, *Geochemische Verteilungsgesetze der Elemente. V. Isomorphie und Polymorphie der Sesquioxyde. Die Lanthaniden-Kontraktion und ihre Konsequenzen*: *Norske vidensk.-akad. Oslo*, v. 5, *Mat.-Nat. Kl.* 1, p. 7.
- Kettelle, B. H., and Boyd, G. E., 1947, The exchange adsorption of ions from aqueous solutions by organic zeolites. IV. The separation of the yttrium group rare earths: *Am. Chem. Soc. Jour.*, v. 69, p. 2800-2812.
- King, A. S., 1928, Temperature classification of the stronger lines of cerium and praseodymium: *Astrophys. Jour.*, v. 68, p. 194-245.
- 1933, Temperature classification of the spectrum of neodymium: *Astrophys. Jour.*, v. 78, p. 9-45.
- 1935, Temperature classification of samarium lines: *Astrophys. Jour.*, v. 82, p. 140-191.
- 1939, Temperature classification of europium lines: *Astrophys. Jour.*, v. 89, p. 377-430.
- 1941, Temperature classification of thulium lines: *Astrophys. Jour.*, v. 94, p. 226-231.
- Meggers, W. F., 1928, Wave lengths and Zeeman effects in yttrium spectra: *U. S. Natl. Bur. Standards Jour. Research*, v. 1, p. 319-341.
- Meggers, W. F., and Scribner, B. F., 1937a, Arc and spark spectra of lutecium: *U. S. Natl. Bur. Standards Jour. Research*, v. 19, p. 31-39.
- 1937b, Arc and spark spectra of ytterbium: *U. S. Natl. Bur. Standards Jour. Research*, v. 19, p. 651-664.

- Milton, Charles, Murata, K. J., and Knechtel, M. M., 1944, Weinschenkite, yttrium phosphate dihydrate, from Virginia: *Am. Mineralogist*, v. 29, p. 92-110.
- Mooney, R. C. L., 1950, X-ray diffraction study of cerous phosphate and related crystals. I. Hexagonal modification: *Acta Crystallographica*, v. 3, p. 337-354.
- Murata, K. J., Rose, H. J., Jr., and Carron, M. K., 1953, Systematic variation of rare earths in monazite: *Geochim. et Cosmochim. Acta*, v. 4, p. 292-300.
- Murata, K. J., Rose, H. J., Jr., Carron, M. K., and Glass, J. J., 1957, Systematic variation of rare-earth elements in cerium-earth minerals: *Geochim. et Cosmochim. Acta*, v. 11, p. 141-161.
- Norris, J. A., and Pepper, C. E., 1952, Quantitative spectrochemical analysis of rare-earth mixtures: *Anal. Chemistry*, v. 24, p. 1399-1403.
- Palache, Charles, Berman, Harry, and Frondel, Clifford, 1951, Dana's system of mineralogy, 7th ed., v. 2: New York, John Wiley and Sons, Inc., 1124 p.
- Peppard, D. F., Faris, J. P., Gray, P. R., and Mason, G. W., 1953, Studies of the solvent extraction behavior of the transition elements. I. Order and degree of fractionation of the trivalent rare earths: *Jour. Phys. Chemistry*, v. 57, p. 294-301.
- Rose, H. J., Jr., Murata, K. J., and Carron, M. K., 1954, A chemical-spectrochemical method for the determination of rare-earth elements and thorium in cerium minerals: *Spectrochimica Acta*, v. 6, p. 161-168.
- Russell, H. N., 1950, The arc and spark spectra of gadolinium: *Optical Soc. America Jour.*, v. 40, p. 550-575.
- Vickery, R. C., 1953, *Chemistry of the lanthanons*: New York, Academic Press, Inc., p. 205.
- Waring, C. L., and Mela, Henry, Jr., 1953, Method for determination of small amounts of rare earths and thorium in phosphate rocks: *Anal. Chemistry*, v. 25, p. 432-435.
- Weaver, Boyd, 1954a, The separation factor. A criterion for evaluation of fractional separation processes: *Anal. Chemistry*, v. 26, p. 474-475.
- 1954b, Fractional separation of rare earths by precipitation with mandelic acid: *Anal. Chemistry*, v. 26, p. 476-478.
- 1954c, Fractional separation of rare earths by oxalate precipitation from homogeneous solution: *Anal. Chemistry*, v. 26, p. 479-480.
- Yost, D. M., Russell, Horace, Jr., and Garner, C. S., 1947, *The rare earth elements and their compounds*: New York, John Wiley and Sons, Inc., p. 42.

Contributions to Geochemistry 1955-57

G E O L O G I C A L S U R V E Y B U L L E T I N 1 0 3 6

*This bulletin was printed
as separate chapters A-N*



UNITED STATES DEPARTMENT OF THE INTERIOR

FRED A. SEATON, *Secretary*

GEOLOGICAL SURVEY

Thomas B. Nolan, *Director*

CONTENTS

[The letters in parentheses preceding the titles designate separately published chapters]

	Page
(A) Rapid field and laboratory method for the determination of copper in soil and rocks, by Hy Almond.....	1
(B) Rapid determination of germanium in coal, soil, and rock, by Hy Almond, Harry E. Crowe, and Charles E. Thompson.....	9
(C) Rapid analysis of silicate rocks, by Leonard Shapiro and W. W. Brannock.....	19
(D) Correlation of dioctahedral potassium micas on the basis of their charge relations, by Margaret D. Foster.....	57
(E) An application of spectrographic microphotometric scanning, by C. L. Waring, Mona Franck, and A. M. Sherwood.....	69
(F) A spectrographic method for determining the hafnium-zirconium ratio in zircon, by C. L. Waring and H. W. Worthing.....	81
(G) X-ray powder data for uranium and thorium minerals, by Clifford Frondel, Daphne Riska, and Judith Weiss Frondel.....	91
(H) The occurrence of minor elements in ash of low-rank coal from Texas, Colorado, North Dakota, and South Dakota, by Maurice Duel and C. S. Annell.....	155
(I) Colorimetric determinations of traces of bismuth in rocks, by F. N. Ward and H. E. Crowe.....	173
(J) Field determination of uranium in natural waters, by F. N. Ward and A. P. Marranzino.....	181
(K) Differential thermal analysis of selected borate minerals, by Robert D. Allen.....	193
(L) A field chromatographic method for determination of uranium in soils and rocks, by Charles E. Thompson and H. W. Lakin.....	209
(M) Model '54 transmission and reflection fluorimeter for determination of uranium with adaptation to field use, by E. E. Parshall and L. F. Rader, Jr.....	221
(N) Fractional precipitation of rare earths with phosphoric acid, by M. K. Carron, C. R. Naeser, H. J. Rose Jr., and F. A. Hildebrand..	253

the 1990s, the number of people in the world who are undernourished has increased from 600 million to 800 million. The number of people who are malnourished has increased from 1.2 billion to 1.5 billion. The number of people who are obese has increased from 100 million to 300 million.

The World Bank has estimated that the cost of malnutrition to the world economy is \$100 billion per year. The cost of obesity to the world economy is \$100 billion per year. The cost of undernourishment to the world economy is \$100 billion per year.

The World Bank has estimated that the cost of malnutrition to the world economy is \$100 billion per year. The cost of obesity to the world economy is \$100 billion per year. The cost of undernourishment to the world economy is \$100 billion per year.

The World Bank has estimated that the cost of malnutrition to the world economy is \$100 billion per year. The cost of obesity to the world economy is \$100 billion per year. The cost of undernourishment to the world economy is \$100 billion per year.

The World Bank has estimated that the cost of malnutrition to the world economy is \$100 billion per year. The cost of obesity to the world economy is \$100 billion per year. The cost of undernourishment to the world economy is \$100 billion per year.

The World Bank has estimated that the cost of malnutrition to the world economy is \$100 billion per year. The cost of obesity to the world economy is \$100 billion per year. The cost of undernourishment to the world economy is \$100 billion per year.

The World Bank has estimated that the cost of malnutrition to the world economy is \$100 billion per year. The cost of obesity to the world economy is \$100 billion per year. The cost of undernourishment to the world economy is \$100 billion per year.

The World Bank has estimated that the cost of malnutrition to the world economy is \$100 billion per year. The cost of obesity to the world economy is \$100 billion per year. The cost of undernourishment to the world economy is \$100 billion per year.

The World Bank has estimated that the cost of malnutrition to the world economy is \$100 billion per year. The cost of obesity to the world economy is \$100 billion per year. The cost of undernourishment to the world economy is \$100 billion per year.

The World Bank has estimated that the cost of malnutrition to the world economy is \$100 billion per year. The cost of obesity to the world economy is \$100 billion per year. The cost of undernourishment to the world economy is \$100 billion per year.

The World Bank has estimated that the cost of malnutrition to the world economy is \$100 billion per year. The cost of obesity to the world economy is \$100 billion per year. The cost of undernourishment to the world economy is \$100 billion per year.

The World Bank has estimated that the cost of malnutrition to the world economy is \$100 billion per year. The cost of obesity to the world economy is \$100 billion per year. The cost of undernourishment to the world economy is \$100 billion per year.

the 1990s, the number of people in the world who are undernourished has increased from 250 million to 800 million.

There are a number of reasons why the world's population is growing so fast. One of the main reasons is that the world's population is becoming younger. In 1990, the world's population was 5.3 billion. By 2000, it was 6.1 billion. By 2010, it is expected to be 6.9 billion. By 2020, it is expected to be 7.6 billion. By 2030, it is expected to be 8.3 billion. By 2040, it is expected to be 8.9 billion. By 2050, it is expected to be 9.6 billion. By 2060, it is expected to be 10.3 billion. By 2070, it is expected to be 10.9 billion. By 2080, it is expected to be 11.5 billion. By 2090, it is expected to be 12.1 billion.

Another reason why the world's population is growing so fast is that the world's population is becoming more urban. In 1990, 40% of the world's population lived in urban areas. By 2000, 50% of the world's population lived in urban areas. By 2010, 58% of the world's population lived in urban areas. By 2020, 65% of the world's population lived in urban areas. By 2030, 72% of the world's population lived in urban areas. By 2040, 78% of the world's population lived in urban areas. By 2050, 84% of the world's population lived in urban areas. By 2060, 89% of the world's population lived in urban areas. By 2070, 93% of the world's population lived in urban areas. By 2080, 96% of the world's population lived in urban areas. By 2090, 98% of the world's population lived in urban areas.

A third reason why the world's population is growing so fast is that the world's population is becoming more educated. In 1990, 50% of the world's population was illiterate. By 2000, 40% of the world's population was illiterate. By 2010, 30% of the world's population was illiterate. By 2020, 20% of the world's population was illiterate. By 2030, 10% of the world's population was illiterate. By 2040, 5% of the world's population was illiterate. By 2050, 2% of the world's population was illiterate. By 2060, 1% of the world's population was illiterate. By 2070, 0.5% of the world's population was illiterate. By 2080, 0.2% of the world's population was illiterate. By 2090, 0.1% of the world's population was illiterate.

A fourth reason why the world's population is growing so fast is that the world's population is becoming more healthy. In 1990, the world's population had a life expectancy of 52 years. By 2000, the world's population had a life expectancy of 57 years. By 2010, the world's population had a life expectancy of 62 years. By 2020, the world's population had a life expectancy of 67 years. By 2030, the world's population had a life expectancy of 72 years. By 2040, the world's population had a life expectancy of 77 years. By 2050, the world's population had a life expectancy of 82 years. By 2060, the world's population had a life expectancy of 87 years. By 2070, the world's population had a life expectancy of 92 years. By 2080, the world's population had a life expectancy of 97 years. By 2090, the world's population had a life expectancy of 102 years.

A fifth reason why the world's population is growing so fast is that the world's population is becoming more mobile. In 1990, 10% of the world's population was mobile. By 2000, 20% of the world's population was mobile. By 2010, 30% of the world's population was mobile. By 2020, 40% of the world's population was mobile. By 2030, 50% of the world's population was mobile. By 2040, 60% of the world's population was mobile. By 2050, 70% of the world's population was mobile. By 2060, 80% of the world's population was mobile. By 2070, 90% of the world's population was mobile. By 2080, 95% of the world's population was mobile. By 2090, 98% of the world's population was mobile.

A sixth reason why the world's population is growing so fast is that the world's population is becoming more affluent. In 1990, 10% of the world's population was affluent. By 2000, 20% of the world's population was affluent. By 2010, 30% of the world's population was affluent. By 2020, 40% of the world's population was affluent. By 2030, 50% of the world's population was affluent. By 2040, 60% of the world's population was affluent. By 2050, 70% of the world's population was affluent. By 2060, 80% of the world's population was affluent. By 2070, 90% of the world's population was affluent. By 2080, 95% of the world's population was affluent. By 2090, 98% of the world's population was affluent.

A seventh reason why the world's population is growing so fast is that the world's population is becoming more educated. In 1990, 50% of the world's population was illiterate. By 2000, 40% of the world's population was illiterate. By 2010, 30% of the world's population was illiterate. By 2020, 20% of the world's population was illiterate. By 2030, 10% of the world's population was illiterate. By 2040, 5% of the world's population was illiterate. By 2050, 2% of the world's population was illiterate. By 2060, 1% of the world's population was illiterate. By 2070, 0.5% of the world's population was illiterate. By 2080, 0.2% of the world's population was illiterate. By 2090, 0.1% of the world's population was illiterate.

A eighth reason why the world's population is growing so fast is that the world's population is becoming more healthy. In 1990, the world's population had a life expectancy of 52 years. By 2000, the world's population had a life expectancy of 57 years. By 2010, the world's population had a life expectancy of 62 years. By 2020, the world's population had a life expectancy of 67 years. By 2030, the world's population had a life expectancy of 72 years. By 2040, the world's population had a life expectancy of 77 years. By 2050, the world's population had a life expectancy of 82 years. By 2060, the world's population had a life expectancy of 87 years. By 2070, the world's population had a life expectancy of 92 years. By 2080, the world's population had a life expectancy of 97 years. By 2090, the world's population had a life expectancy of 102 years.

A ninth reason why the world's population is growing so fast is that the world's population is becoming more mobile. In 1990, 10% of the world's population was mobile. By 2000, 20% of the world's population was mobile. By 2010, 30% of the world's population was mobile. By 2020, 40% of the world's population was mobile. By 2030, 50% of the world's population was mobile. By 2040, 60% of the world's population was mobile. By 2050, 70% of the world's population was mobile. By 2060, 80% of the world's population was mobile. By 2070, 90% of the world's population was mobile. By 2080, 95% of the world's population was mobile. By 2090, 98% of the world's population was mobile.